

Surface engineering of zinc sulphide film for augmenting the performance of polycrystalline silicon solar cells

V. K. Gobinath^a, R. Rajasekar^{b,*}, C. Moganapriya^b, A. Manju Sri^c, G. Raja^d,
P. Sathish Kumar^e, S. K. Jaganathan^{f,g,h}

^a*Department of Mechatronics Engineering, Kongu Engineering College, Perundurai, Tamil Nadu, India – 638060*

^b*Department of Mechanical Engineering, Kongu Engineering College, Perundurai, Tamil Nadu, India – 638060*

^c*Department of Chemical Engineering, Kongu Engineering College, Perundurai, Tamil Nadu, India - 638060*

^d*Department of Mechanical Engineering, Velalar college of Engineering and Technology, Erode, India – 638012*

^e*Mining Engineering, Indian Institute of Technology Kharagpur, Kharagpur, India - 721302*

^f*Bionanotechnology Research Group, Ton Duc Thang University, Ho Chi Minh City, Vietnam;*

^g*Faculty of Applied Sciences, Ton Duc Thang University, Ho Chi Minh City, Vietnam;*

^h*Department of Engineering, Faculty of Science and Engineering, University of Hull, HU6 7RX, United Kingdom*

The current work focused on enhancing solar cell's Power Conversion Efficiency (PCE) while using zinc sulphide (ZnS) material as Anti-Reflective Coating (ARC). The ZnS layers were deposited over the solar cell surface by RF sputtering technique. The coating was performed in argon gas atmosphere with sputtering time such as 10, 20, 30 & 40 min represented as S-I, S-II, S-III and S-IV respectively. The power conversion efficiency of ZnS coating on polycrystalline silicon solar cells was studied by evaluating optical properties, electrical characteristics, structure morphology and temperature study. It is observed that the S-III coating exhibits optimum hall mobility (μ), improved carrier concentration (N) and electrical resistivity (ρ) and the measured values are $12.88 \text{ cm}^2 \text{V}^{-1} \text{s}^{-1}$, $3.98 \times 10^{-3} \Omega\text{-cm}$ and $21.88 \times 10^{20} \text{ cm}^{-3}$ respectively. The maximum PCE of 17.39% and 19.12% are obtained for S-III coating at open source condition and controlled source condition respectively. The effect of operating temperature on ZnS coated solar cells at both open source and controlled source condition is also investigated. The results revealed that the ZnS can be reliable ARC for improving the power conversion efficiency of solar cells.

(Received March 27, 2021; Accepted July 2, 2021)

Keywords: Sustainable energy, Polycrystalline silicon solar cells, Reflection loss, Zinc sulphide, Power conversion efficiency

1. Introduction

The depletion of fossil fuels and their environmental concerns such as increase in global warming, rise in sea level, air and water pollution made the researchers to focus on the alternative sources of energy. The sustainable energy sources could be modified to address the disadvantages of traditional non-renewable energy sources. Solar energy is identified as the most promising feature to generate electricity which is clean, renewable and eco-friendly. As per the survey, solar energy is capable of supplying energy twice than that of non-renewable energy consumed in a year. In the production of clean electrical power, photovoltaic cells play a significant role [1]. For

* Corresponding author: rajasekar.cr@gmail.com

<https://doi.org/10.15251/CL.2021.187.375>

the past 10 years, photovoltaic industries are grown by 30% in excess. Researchers have been working in the field of solar cells to reduce optical losses occurred during generation of electricity. Silicon solar cells contribute to 90% of the photovoltaic solar cells in commercial market [2]. Silicon solar cells are very stable, simple fabrication and less harmful to environment than the other solar based cells [3]. Silicon solar cells are very efficient and the silicon is a semiconductor material that is abundantly available in earth. In order to obtain maximum Power Conversion Efficiency (PCE), the losses such as optical and reflection losses should be eliminated for increasing the absorption property of solar cells [4]. The maximum power conversion efficiency can be achieved by utilizing maximum amount of sun light reflected over the surface of solar cells [5]. The reflection losses might be reduced by coating the surface of solar cells with anti-reflective coatings (ARCs) [6, 7]. The naturally available materials such as Zirconia and Monazite in silica sand and chemically incorporated materials like Al_2O_3 , SiO_2 , TiO_2 , SiO , ZnO , SiN_x are commonly used ARC's. These anti-reflection coating materials possess high light trapping ability. Zinc sulphide (ZnS) was preferred for solar photovoltaic thin film devices as it minimizes reflection losses and less toxic. ZnS is a semiconductor material that plays a vital role in visible spectrum devices as it has an energy bandgap of 3.7 eV [8-10].

The different methods have been implemented in coating thin film solar cells such as spray pyrolysis [11, 12], sol gel method [13, 14], sputtering [15, 16] and pulsed laser deposition method [17, 18]. As seen, RF magnetron sputtering is very reliable and also provides smooth and uniform coating throughout. The thin films coated by this technique are highly adherent, self-sustainable and efficient to transfer for industrial purpose [15]. The factors such as increased surface temperature, large size of grains, film damage due to radiation and increased bombardment affects the substrate [19]. However, the thin coated films produced by RF sputtering method has many advantages as it provides optimum electrical and optical properties [20].

In this research work, zinc sulphide (ZnS) was employed for developing ARCs on polycrystalline silicon solar cell. The ZnS thin-films were coated through the RF- sputter coating over the silicon solar cell surface with different sputtering time period. The structural, optical characteristics, electrical properties and temperature analysis of ZnS deposited on solar cells were reported. From this research work, 30 minutes (S-IV) of ZnS coated silicon solar cells exhibited maximum PCE at controlled and open source conditions.

2. Experimental part

2.1. Materials and deposition techniques

The zinc sulphide (powdered form) with 99% purity was brought from Sigma Aldrich, India. The polycrystalline Si solar cell having specification of 52 mm \times 38 mm was purchased from Yixing JS Solar Co., Ltd., China. Thus the obtained materials were utilized in the process of coating after they were surface engineered. During the RF sputtering process, a solid target in pellet form is required for coating. ZnS in the form of pellet was deposited over the surface of solar cells by RF- sputter coating technique. A solid target was developed by the process of pelletizing on applying mechanical load on the mild steel die. Designing of mild steel die and its components such as base plate, male and female units was modeled using Creo. The surface of base plate was coated with Ni for the ease separation of solid target. The ZnS solid pellet was produced using universal testing machine (UTM) by applying vertical load of 1400 MPa on the mild steel die. The weight of the solid pellet produced is approximately 14.5g with a diameter of 5 cm and thickness of 0.5cm. The solar cells were cleaned using ethanol before depositing ZnS thin films. The ZnS films were deposited over the cells by RF- sputter coating method. The ZnS solid target and cleaned polycrystalline silicon solar cells are placed in RF sputter coating machine. The surface contamination on the solar cells and solid target were cleaned by the process of pre-sputtering for 10 min. The different coating time such as S-I (10 min), S-II (20 min), S-III (30 minutes) and S-IV (40 min) were employed during ZnS coating. The parameters specified during the sputter coating operation are as follows, Pressure of vacuum chamber: 6×10^{-2} mbar, Distance at the interface between substrate and solid target: 5 cm, Radio Frequency (RF) Power: 300 W, Sputter gas: Argon. The preparation of solid target and deposition of ZnS was illustrated in Fig. 1.

2.2. Characterizations

The materials used in coating surface of the solar cells are characterized and analyzed by using different characterization methods. X-Ray Diffraction (XRD) procedure was utilized to interpret crystal structures and microstructural properties of ZnS. The morphology of surface and atomic structures are characterized by High Resolution - Transmission Electron Microscope (HR-TEM). Field Emission Scanning Electron Microscopy (FE-SEM) technique was utilized to study morphology of the surface, chemical composition and thickness of both non-coated and ZnS coated cells. The optical behavior of the ZnS coated solar cells were examined by Ultraviolet visible near infrared spectrophotometer (UV-Vis-NIR). Four-probe testing method was engaged to evaluate the hall mobility and electrical resistivity. Keithley 2450 meter is employed to determine the current-voltage relation of both ZnS coated and bare solar cells. Thermal behavior of both bare and ZnS coated silicon solar cells were interpreted using thermal image camera.

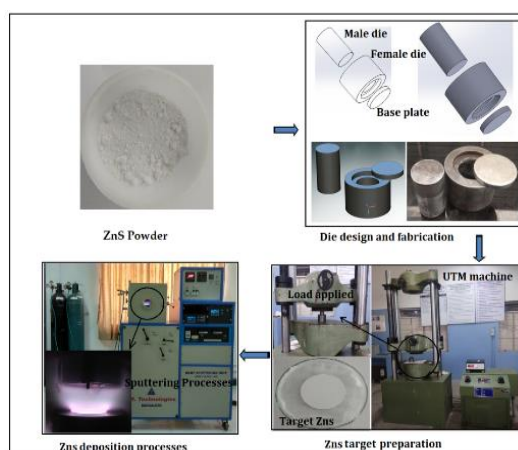


Fig. 1. ZnS target preparation and deposition processes.

3. Results and discussion

The pattern obtained from X-Ray diffraction of ZnS (in powder form) is shown in Fig.2. From figure, it is clearly understood that most of the peaks diffracted were correlated with the standard structure of ZnS (JCPDS card No.39-1363). The purchased ZnS diffraction peak's position is matched with the standard data (Fig.2).

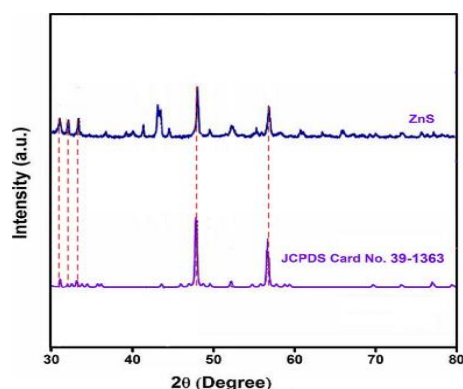


Fig. 2. XRD pattern of ZnS.

The size and shape of each grains were explored through High Resolution - Transmission Electron Microscope (HR-TEM). The ZnS powder is mixed with C_2H_5OH (ethanol) and it is

deposited over the carbon film using copper grid. Then the grid is located in HR-TEM under the maximum voltage of 200 kV. The shape and size of the ZnS powder is clearly depicted in Fig.3 (a&b). It is observed that the particles formed are in the range of 98 – 184 nm with different shapes such as circle, sphere and elliptical having irregular contours.

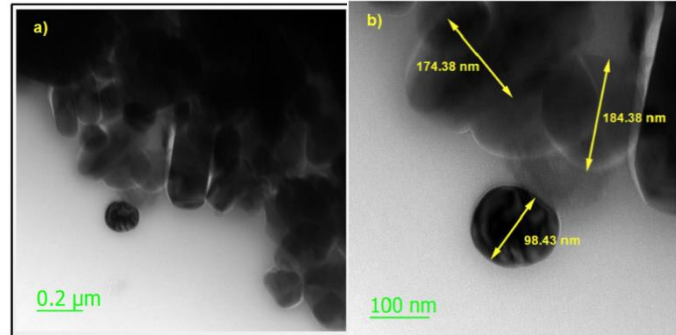


Fig. 3 TEM photographs of ZnS powder.

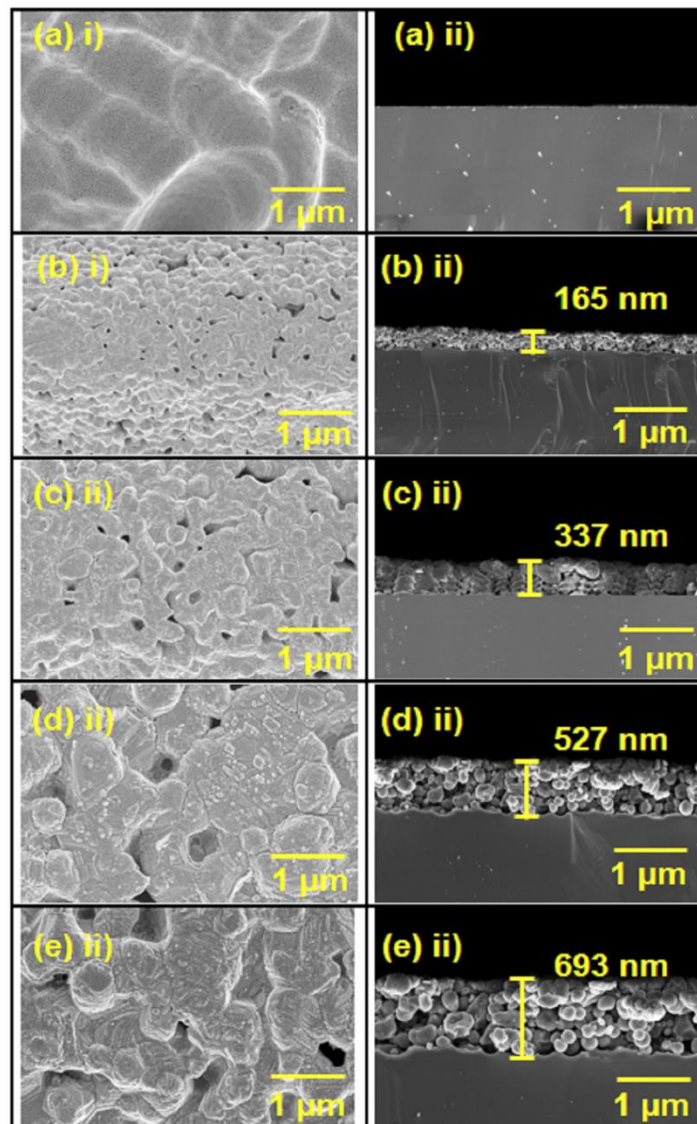


Fig. 4 FE-SEM image of bare cell a) (i & ii) and ZnS coated solar cells; b) S-I (i & ii), c) S-II (i & ii), d) S-III (i & ii), and e) S-IV (i & ii).

The morphology of ZnS coating films was analyzed for all coating times from S-I to S-IV min. FE-SEM was employed to examine the surface texture and their thickness at cross section of ZnS coated films. The surface morphology and their cross section images of both non-coated and ZnS coated silicon cells revealed from FE-SEM were depicted in Fig.4 (a-e). The observed grains of ZnS were wide and dense. The grain size at the film surface depends on sputtering time not the nature of substrate [21]. During the process of deposition, cluster grains are formed on the solar cell substrate which was confirmed by the presence of crystalline agglomeration. The film thickness of ZnS thin-film at different sputtering times of S-I to S-IV is 165, 337, 527, and 693 nm respectively. From the observations, it is identified that ZnS film thickness is proportional to coating time.

The compositions of different elements present in ZnS thin film depositions were assessed using Energy Dispersive X-Ray Analysis (EDAX) for the coated film of S-III min. The results were shown in Fig. 5. From the EDAX analysis, it is clear that large number of well-defined peaks is in correlation with Zn and S, as it proves that the ZnS comprised of Zn and S.

The optical characteristics of ZnS coated silicon based solar cells were illustrated in Fig. 6. A high transmittance of about 300 - 800 nm was achieved while coating the substrate of the solar cells with ZnS. From fig.6 it is clear that the maximum transmittance of 85% is obtained during ZnS coating at S-III min when compared to other samples. During ZnS coating, it is seen that the value of optical transmittance rises gradually from S-I to S-III min and there is a decrease in transmittance for S-IV min of coating. It shows the evidence that the optimization of thickness during the anti-reflective coating plays a vital role in coating efficiency, reflection losses and transparency [22]. Further, there is a decrease in transmittance percentage for S-IV min is because of the aggregation of coating material due to increased scattering of light.

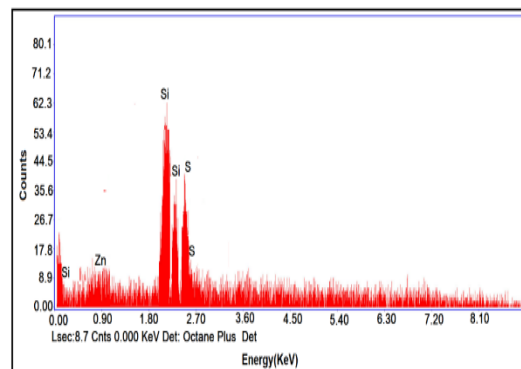


Fig. 5 EDAX of ZnS nano films deposited at S-III min duration on solar cell.

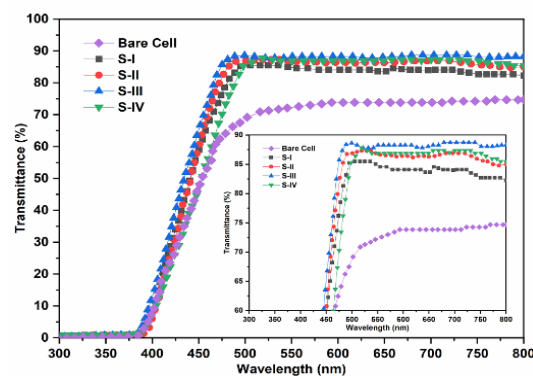


Fig. 6 Optical transmittance characteristics of ZnS coated and bare polycrystalline Si solar cells

Fig. 7 illustrates the electrical properties such as hall mobility (μ), carrier concentration (N) and resistivity (ρ) of both ZnS coated at different sputtering time and uncoated silicon solar cell. From the Fig.6, it is noted that at sputtering time S-III min there is a reduction of resistivity of $3.98 \times 10^{-3} \Omega\text{-cm}$ while comparing with uncoated solar cell which has $8.73 \times 10^{-3} \Omega\text{-cm}$. As the existence of Zn and S concentration in ZnS coated solar cells leads to the reduction of electrical resistivity. The electrical conductivity increases with the reduction of resistivity which is same as that of previous work [22]. In addition, increasing coating time to S-IV min the electrical resistivity of solar cell increases to $4.02 \times 10^{-3} \Omega\text{-cm}$. The solar cells electrical resistivity is associated with thickness of coating [22]. It is also observed from Fig.7 that the graphs of hall mobility and carrier concentration are proportional. The hall mobility is increased from ~ 7.33 to $12.88 \text{ cm}^2\text{V}^{-1}\text{s}^{-1}$ and the carrier concentration also increase from 15.1×10^{20} to $21.88 \times 10^{20} \text{ cm}^{-3}$ with a rise in the coating time from S-I to S-III min. Hall mobility increases with the thickness of coating and this may be due to the reduction of grain boundaries [23, 24]. If the sputtering time is increased to S-IV min, it is observed that the hall mobility and carrier concentration are reduced to $11.99 \text{ cm}^2 \text{V}^{-1}\text{s}^{-1}$ and $20.98 \times 10^{20} \text{ cm}^{-3}$ respectively.

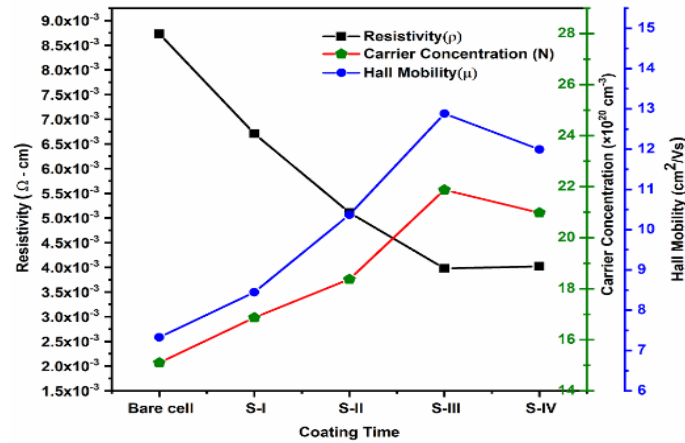


Fig. 7. Electrical resistivity (ρ), carrier concentrations (N) and Hall mobility (μ) of the uncoated cell and ZnS coated solar cells with different sputtering periods of S-I to S-IV min.

The power conversion efficiency of ZnS coated solar cells at different sputtering time were compared with the uncoated solar cell at both open source and controlled source conditions. At open source condition the efficiency of both uncoated and ZnS coated solar cells were examined nearly at 12.30 pm. I-V plots demonstrating the performance of ZnS nano layer coated solar cells of size $5.2 \text{ cm} \times 3.8 \text{ cm}$ at open source condition is shown in Fig. 8. The power conversion efficiency of ZnS coated cell is sufficient as derived in terms of physical variables shown in Table 1. It is clear that open circuit voltage and short circuit photocurrent density was maximum for ZnS coated cell than uncoated solar cells. Exceptionally, the sputtering time of S-III min resulted an increased PCE of 17.39% than the uncoated solar cell with PCE of 14.86%. Further increase in sputtering time leads to decrease in the J_{sc} value so that the PCE also reduced.

Table 1. I-V performance at open source conditions.

Solar cell	J_{sc} (mA/cm ²)	V_{oc} (V)	Fill Factor (%)	PCE (%)
Bare cell	32.1	0.63	76.1	14.86
S-I	33.0	0.632	76.2	15.35
S-II	35.1	0.638	76.8	16.63
S-III	36.1	0.647	77.1	17.39
S-IV	35.5	0.639	76.9	16.87

Fig. 9 depicts the experimental setup at controlled source conditions to examine I-V relation. A solar simulator is designed with the neodymium daylight lamp for supplying radiation and the level of radiation is regulated using AC regulator. There are no periodic fluctuations in controlled source conditions which happen in open source condition. The radiation from neodymium lamp is measured using pyrometer. The distribution of temperature over surface of both uncoated and ZnS coated solar cells are examined using IR thermal imaging. The current-voltage (I-V graphs) determining the photovoltaic performance at controlled source conditions of both bare and ZnS coated cells was depicted in Fig. 10. In controlled source conditions, illumination of neodymium light radiation of 1000 W/m^2 is used.

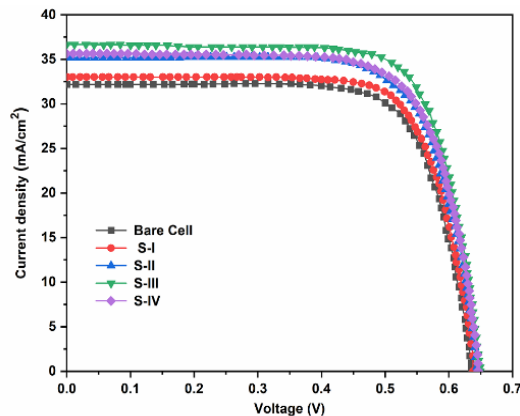


Fig. 8 I-V performance of bare cell and ZnS coated solar cell under open source conditions.

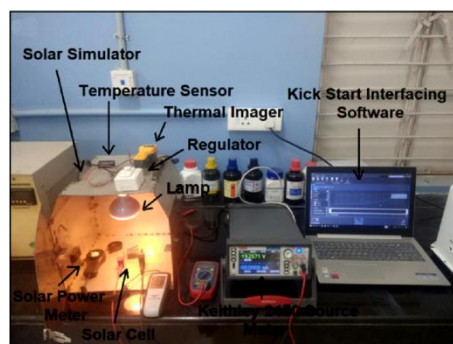


Fig. 9 Controlled source condition experimental setup.

The power conversion efficiency of ZnS coated and bare silicon solar cells are assessed from current-voltage graph as shown in Table 2. The uncoated cell delivers a power conversion efficiency of 15.88% ($V_{oc} = 0.632 \text{ V}$, $J_{sc} = 33.518 \text{ mA/cm}^2$, $FF = 0.75$). The ZnS coated at S-III min exhibits remarkable $V_{oc} = 0.646 \text{ V}$, $J_{sc} = 38.5 \text{ mA/cm}^2$, and $FF = 76.9\%$. The increment of power conversion efficiency from 15.88 to 19.12% is due to the maximum J_{sc} and V_{oc} . Anyhow, ZnS coating at S-III min exhibits better PCE than uncoated and other three coated solar cells. In addition, at S-IV min sputtering time there is a decline in J_{sc} and V_{oc} along with that PCE also decreases as stated in Table 2 and Fig. 10.

Table 2. I-V performance at controlled source condition.

Solar cell	J_{sc} (mA/cm ²)	V_{oc} (V)	Fill Factor (%)	PCE (%)
Bare cell	33.51	0.632	75	15.88
S-I	35.12	0.633	76.1	16.91
S-II	36.57	0.635	76.2	17.69
S-III	38.5	0.646	76.9	19.12
S-IV	37.2	0.641	76.5	18.24

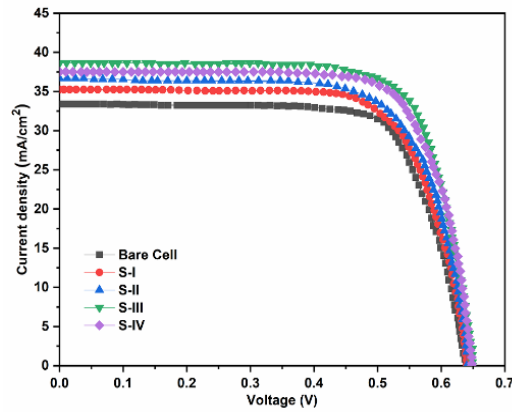


Fig. 10 I-V performance of bare cell and ZnS coated solar cell under controlled source conditions.

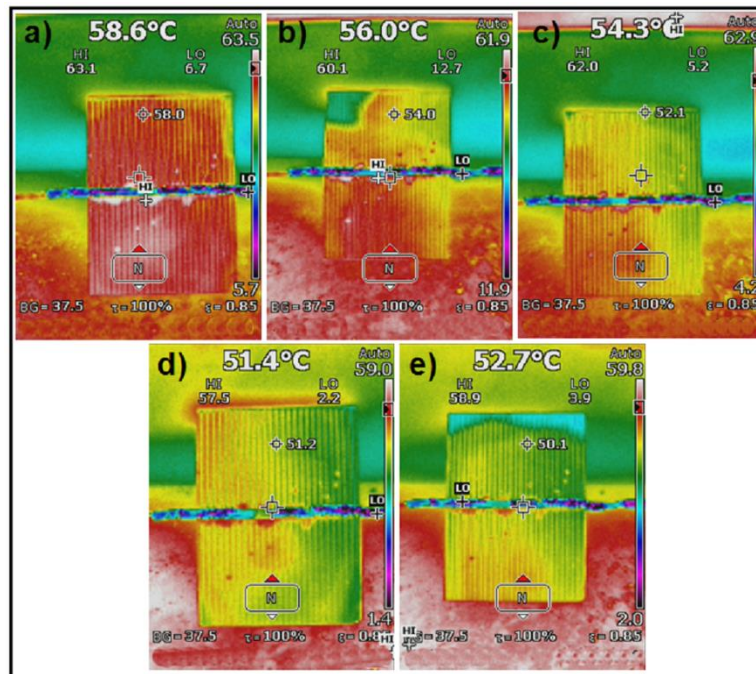


Fig. 11 (i) Temperature exploration of ZnS coated and bare polycrystalline Si solar cells under open source conditions.

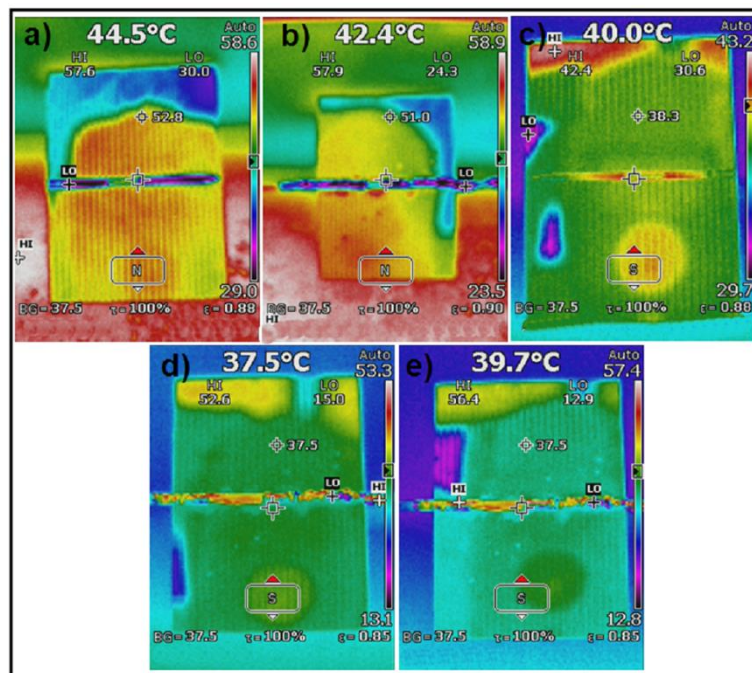


Fig. 11 (ii) Temperature exploration of ZnS coated and bare polycrystalline Si solar cells under closed source conditions.

The surface temperature of both uncoated and ZnS coated solar cells are examined at open source and control source conditions. As the temperature of solar panels increases, PCE decreases considerably [25, 26]. IR thermal imaging is used for evaluating the temperature without any contact with target. The data transmission is easy and quick due to visual images associated with infrared technology.

Fig. 11 illustrates the thermal images of bare cell (a), S-I (b), S-II (c), S-III (d), and S-IV (e) min of ZnS coated solar panels at open source (Fig. 11(i)) and controlled source (Fig. 11(ii)) conditions. It is observed that the S-III min exhibits lower temperature of 37.5°C at open source condition and 51.4 °C at closed source condition than uncoated and ZnS coated solar cells. The heat flux is high for solar cells due to improved light scattering and so thermal image transparency is reduced for anti-reflective coatings. It is clearly seen that the PCE of solar cells are high at low temperature.

4. Conclusions

The coating of ZnS thin films were successfully incorporated on top surface of polycrystalline silicon solar cell through RF-sputter coating method. Sputter-coated ZnS silicon solar cell at S-III min reveals maximum transmittance of 85%. The high efficiency of about 17.39% for open source conditions and 19.12% for controlled conditions have been attained by S-III min of ZnS deposition, which is higher than the uncoated cell and ZnS coated solar cells at different coating time. The temperature results depicts that minimum temperature is achieved by S-III min coated cell i.e. 37.5°C for open source conditions and 51.4°C for controlled source conditions. From these results, it is evidently discussed that PCE of solar cells varies inversely with operating temperature. The increase in power conversion efficiency of solar cells leads to improvement in optical transmittance at surface.

Acknowledgements

The authors are thankful to the management of Kongu Engineering College, Perundurai, Erode for providing necessary research facilities.

References

- [1] R. Sharma, G. Amit, V. Ajit, **9**(2), 2017.
- [2] A. Aberle, *Advances in OptoElectronics* **2007**, (2007).
- [3] N. F. Habubi, R. A. Ismail, K. A. Mishjil, K. I. Hassoon, *Silicon*, 2018.
- [4] A. Uzum, M. Kuriyama, H. Kanda, Y. Kimura, K. Tanimoto, H. Fukui, T. Izumi, T. Harada, S. Ito, *International Journal of Photoenergy* **2017**, (2017).
- [5] D.-W. Kang, J.-Y. Kwon, J. Shim, H.-M. Lee, M.-K. Han, *Solar Energy Materials and Solar Cells* **101**, 2012.
- [6] S.-Y. Lien, D.-S. Wu, W.-C. Yeh, J.-C. Liu, *Solar Energy Materials and Solar Cells* **90**(16), 2006.
- [7] Ö. Kesmez, E. Akarsu, H.E. Çamurlu, E. Yavuz, M. Akarsu, E. Arpaç, *Ceramics International* **44**(3), 2018.
- [8] S. Tec-Yam, J. Rojas, V. Rejón, A. Oliva, *Materials Chemistry and Physics* **136**(2-3), 2012.
- [9] J. Borah, K. Sarma, *Acta Physica Polonica-Series A General Physics* **114**(4), 2008.
- [10] L.-X. Shao, K.-H. Chang, H.-L. Hwang, *Applied Surface Science* **212**, 2003.
- [11] M. H. Sayed, E. V. Robert, P. J. Dale, and L. Gütay, *Thin Solid Films* **669**, 2019.
- [12] A. Tombak, T. Kilicoglu, Y. S. Ocak, *Renewable Energy*, 2019.
- [13] D. Chen, *Solar Energy Materials and Solar Cells* **68**(3-4), 2001.
- [14] L. Ye, Y. Zhang, X. Zhang, T. Hu, R. Ji, B. Ding, B. Jiang, *Solar Energy Materials and Solar Cells* **111**, 2013.
- [15] C. Besleaga, L. Ion, S. Antohe, *Romanian Reports in Physics* **66**(4), 2014.
- [16] D. Dimova-Malinovska, N. Tzenov, M. Tzolov, L. Vassilev, *Materials Science and Engineering: B* **52**(1), 1998.
- [17] C.-Q. Luo, F. C.-C. Ling, M.A. Rahman, M. Phillips, C. Ton-That, C. Liao, K. Shih, J. Lin, H. W. Tam, A. B. Djurišić, *Applied Surface Science* **483**, 2019.
- [18] S.-H. Yuan, S.-L. Ou, C.-M. Chen, S.-Y. Huang, B.-W. Hsiao, D.-S. Wu, *Ceramics International* **45**(1), 2019.
- [19] J. Vossen, *Journal of Vacuum Science and Technology* **8**(5), 1971.
- [20] S. Rahmane, M. S. Aida, M. A. Djouadi, N. Barreau, *Superlattices and Microstructures* **79**, 2015.
- [21] P. Prepelita, M. Filipescu, I. Stavarache, F. Garoi, D. Craciun, *Applied Surface Science* **424**, 2017.
- [22] G. V. Kaliyannan, S. V. Palanisamy, M. Palanisamy, M. Chinnasamy, S. Somasundaram, N. Nagarajan, R. Rathanasamy, *Applied Nanoscience*, 2019.
- [23] H. Du, M. Lv, J. Meng, W. Zhu, *Applied optics* **55**(34), 2016.
- [24] Y. Liu, Y. Li, H. Zeng, *Journal of Nanomaterials* **2013**, 2013.
- [25] G. V. Kaliyannan, S. V. Palanisamy, M. Palanisamy, M. Subramanian, P. Paramasivam, R. Rathanasamy, *Materials Science-Poland* **37**(3), 2019.
- [26] G. V. Kaliyannan, S. V. Palanisamy, R. Rathanasamy, M. Palanisamy, S. K. Palaniappan, M. Chinnasamy, *Journal of Materials Science: Materials in Electronics* **31**(3), 2020.